Dynamic modes of quasispherical vesicles: Exact analytical solutions

M. Guedda,[1,*] M. Abaidi,[1] M. Benlahsen,[2] and C. Misbah[3]
[1]*Université de Picardie Jules Verne, LAMFA CNRS UMR 7352, Amiens F-80039, France*
[2]*Université de Picardie Jules Verne, LPMC, Amiens F-80039, France*
[3]*Université Grenoble I, CNRS, Laboratoire Interdisciplinaire de Physique, UMR 5588, Grenoble F-38041, France*
(Received 2 August 2012; revised manuscript received 18 October 2012; published 26 November 2012)

In this paper we introduce a simple mathematical analysis to reexamine vesicle dynamics in the quasispherical limit (small deformation) under a shear flow. In this context, a recent paper [Misbah, Phys. Rev. Lett. **96**, 028104 (2006)] revealed a dynamic referred to as the vacillating-breathing (VB) mode where the vesicle main axis oscillates about the flow direction and the shape undergoes a breathinglike motion, as well as the tank-treading and tumbling (TB) regimes. Our goal here is to identify these three modes by obtaining explicit analytical expressions of the vesicle inclination angle and the shape deformation. In particular, the VB regime is put in evidence and the transition dynamics is discussed. Not surprisingly, our finding confirms the Keller-Skalak solutions (for rigid particles) and shows that the VB and TB modes coexist, and whether one prevails over the other depends on the initial conditions. An interesting additional element in the discussion is the prediction of the TB and VB modes as functions of a control parameter Γ, which can be identified as a TB-VB parameter.

DOI: 10.1103/PhysRevE.86.051915 PACS number(s): 87.16.D−, 87.19.U−, 47.15.G−, 47.60.Dx

I. INTRODUCTION

The aim of this investigation is to solve exactly a highly nonlinear system of coupled ordinary differential equations that is derived to model the dynamics of a vesicle subject to unbounded steady shear flow. Vesicles (also known as fluid membranes) and red blood cells (RBCs) have been, and remain, the subject of extensive studies (see [1–39] and the references therein). Nowadays there is an increasing interest in this research activity in different disciplines ranging from biology to applied mathematics. It is found that vesicles and RBCs display at least two main types of dynamics: (i) the tank-treading (TT) mode, where the vesicle deforms into a prolate ellipsoid inclined at a stationary angle $0 < \psi < \pi/4$ with the flow direction, while its membrane undergoes a tank-treading motion, and (ii) the tumbling (TB) mode, in which the membrane flips like a rigid body, provided its initial shape is not spherical. These two types of motion are predicted by the Keller-Skalak (KS) theory [1] which assumed a fixed ellipsoidal vesicle shape.

To focus the discussion, the dynamics of vesicles and RBCs under a shear flow depends on three dimensional parameters (see, for example, [24,26]): (i) The first is the excess area relative to a sphere $\Delta = (A - 4\pi r_0^2)/r_0^2$, where A is the vesicle area and r_0 is the effective vesicle radius or the radius of a sphere having the same volume V as the vesicle ($[r_0 = (3V/4\pi)^{1/3}]$. The excess area Δ is non-negative and vanishes for a sphere. (ii) The second is the ratio $\lambda = \eta_{\text{int}}/\eta_{\text{ext}}, \eta_{\text{int}}$ and η_{ext} being the viscosities of the internal and the external fluids, respectively. (iii) The third is the capillary number $C_a = \eta_{\text{ext}}\dot{\gamma} r_0^3/\kappa$, where $\dot{\gamma}$ and κ are the shear rate and the membrane bending rigidity, respectively.

In addition to the TT and TB regimes, an intermediate regime, which has attracted the attention of many researchers, has been presented by one the authors [12]. In this regime the main axis of the vesicle oscillates about the flow direction, whereas its shape makes a breathing motion. This regime, which is called the vacillating-breathing (VB) mode (later also described as trembling or swinging), has undergone considerable numerical and experimental investigation, which constitutes the initial motivation of the present work.

The theory for the VB dynamic mode is based on the small excess area approximation (i.e., almost spherical vesicles or the quasispherical regime) and on spherical harmonic expansions of the shape deviation. Neglecting membrane thermal undulations, at leading order ($\varepsilon = \sqrt{\Delta}$ is the small expansion parameter) Misbah [12] derived the following coupled nonlinear ordinary differential equations:

$$\begin{aligned} \frac{d\mathcal{R}}{dt} &= h\left[1 - 4\frac{\mathcal{R}^2}{\Delta}\right]\sin(2\psi), \\ \frac{d\psi}{dt} &= -\frac{1}{2} + \frac{h}{2\mathcal{R}}\cos(2\psi), \end{aligned} \tag{1}$$

where the unknowns ψ and $\mathcal{R}$ represent, respectively, the vesicle inclination angle and its shape deformation. Here, lengths are reduced by the vesicle radius r_0 and time by $\dot{\gamma}^{-1}$. System (1) gives the temporal evolutions of ψ and $\mathcal{R}$ as functions of Δ and the parameter $h = 60\sqrt{2\pi/15}/(32 + 23\lambda)$ (or the viscosity ratio λ). This is a generalization of the KS theory which assumed a fixed ellipsoid shape, $\mathcal{R} \equiv \sqrt{\Delta}/2$. It is noteworthy that system (1) is free of C_a. As mentioned in [24], the approach of [12] has truncated the expansion of the evolution equations about a spherical shape to leading order (see also [13]). As a consequence, C_a is scaled out from the evolution equations, and only λ and Δ remain. The insensitivity to C_a of the vesicle tilt angle in a shear flow was also reported numerically even for a large enough deformation [2,5,6]. In [15] it is indicated that the theory of Misbah corresponds formally to $C_a \to \infty$. Including higher-order terms leads to the appearance of C_a in the equations [15,23,24].

In [12] the author showed that system (1) has a critical viscosity ratio

$$\lambda_c = -32/23 + (120/23)\sqrt{2\pi/15\Delta}, \tag{2}$$

*guedda@u-picardie.fr

which separates the TT and TB regimes. More precisely, system (1) was integrated numerically for different values of the parameter h and for different initial conditions $\psi(0)$ and $\mathcal{R}(0)$. It is observed that for $\lambda > \lambda_c$, or, equivalently, $h < h_c = \sqrt{\Delta}/2$, the TB mode occurs and coexists with the VB mode. Each mode has its own basin of attraction. Recently, several studies have elucidated this point further [13,14,16,17,19,22]. For $h < h_c$ a linear stability analysis showed that the frequency ω of oscillation about the fixed point $\psi_0 = 0$, $\mathcal{R}_0 = h$ is purely imaginary. This makes it possible, from the mathematical point of view, to have closed orbits around $(0,h)$. By including higher-order terms, it is found that the frequency ω acquires a nonzero real part [16], and the VB mode becomes a limit cycle. Here, we shall see analytically that for $h < h_c$ all solutions are periodic at the leading order, in agreement with the numerical solutions presented in [12].

The overall objective of the present work is, in addition to these numerical investigations, to present the discovery of all exact analytical solutions to system (1), and investigate in detail the dynamical features of quasispherical vesicles. This is useful for interpreting experiments and for testing or developing numerical schemes [27]. In particular, we shall exhibit exact expressions for the vesicle inclination angle and its shape deformation, which lead naturally to the physical properties predicted in [12,14,19]. More importantly, exact solutions may provide simple means to (more realistically) describe the vesicle dynamics, to delineate the regions of existence of the TB and VB modes, and to probe the rheological properties of vesicles. Moreover, this exact solution can be used as a starting basis for an analytical analysis (possibly perturbative) of more complex situations.

This paper is organized as follows. Section II deals with a brief description of the small deformation theory. Section III is devoted to the main results. Vesicle dynamics are discussed in Sec. IV and the basins of attraction of each regime are investigated in Sec. V. Finally, the conclusions is presented in Sec. VI.

II. QUASISPHERICAL APPROACH

For convenience of the readers, we give here a brief description of a vesicle model in the small deformation regime. The present description is based on the papers [12,19]. The vesicle, which is supposed as single, is submitted to a linear shear flow $\mathbf{u}_0 = (\dot{\gamma} y,0,0)$, where $\dot{\gamma}$ is the shear rate. $\dot{\gamma}^{-1}$ will be used as the time unit ($t \to \dot{\gamma} t$). The flow outside (and inside) the vesicle is described by the Stokes equations

$$\eta \nabla^2 \mathbf{u} = \nabla p, \tag{3}$$

where $\mathbf{u}$ and p are the velocity and the pressure fields, respectively. The Reynolds number is assumed to be negligible. The viscosity $\eta = \eta_{\text{int}}$ for the fluid encapsulated by the vesicle and $\eta = \eta_{\text{ext}}$ for the suspending medium. The fluids are assumed to be incompressible,

$$\nabla \cdot \mathbf{u} = 0. \tag{4}$$

The vesicle deformation is described by the radial position r of the vesicle interface, which can be parametrized by

$$r = r_0[1 + f(\theta,\phi,t)], \tag{5}$$

where f is the deviation of the vesicle shape from a sphere depending on the angular coordinates and r_0 is the effective vesicle radius. The shape deviation is a real function and is assumed to be small; $f \sim O(\varepsilon)$, $\varepsilon \ll 1$.

One of the most powerful methods in investigating the vesicle deformations is the spherical harmonic parametrization. Indeed, within this approach, a complicated physical phenomenon is replaced by a simpler formulation that is amenable to mathematical treatment. Technical details will not be presented in this paper. Here, we only sketch the principle. In the following the spatial variables are rescaled by r_0. The function f is expanded into series of scalar spherical harmonics,

$$f = \sum_{n=0}^{\infty} \sum_{m=-n}^{m=n} F_{nm}(t) \mathcal{Y}_n^m(\theta,\phi), \tag{6}$$

where the functions $\mathcal{Y}_n^m$ are the usual spherical harmonics and F_{nm} are unknown time-dependent amplitudes. The constraint on the fixed total area serves to relate the amplitude of the shape perturbation f and the excess area Δ [3,4,13,23]:

$$\begin{aligned} \Delta &= \int \frac{r^2}{\mathbf{e}_r \cdot \mathbf{n}} \sin\theta \, d\theta \, d\phi - 4\pi \\ &= \sum_n \sum_{m=-n}^{m=n} |F_{nm}(t)|^2 \frac{(n+2)(n-1)}{2}, \end{aligned} \tag{7}$$

where $\mathbf{e}_r$ and $\mathbf{n}$ are the unit radial and outward unit normal vectors, respectively. Third- and higher-order terms in F_{nm} are neglected. From (7) we may deduce that the appropriate small parameter ε is given by $\varepsilon = \sqrt{\Delta}$.

By the linearity of the Stokes equations, the total velocity field outside the vesicle, $\mathbf{v}$, can be written as $\mathbf{v} = \mathbf{u}_0 + \mathbf{u}$, where $\mathbf{u}$ is the unknown perturbation of the field due to the presence of the vesicle. Likewise, we write for the velocity field within the vesicle $\overline{\mathbf{v}} = \boldsymbol{\Omega} \times \mathbf{r}/2 + \overline{\mathbf{u}}$, where $\boldsymbol{\Omega}$ is the vorticity. Following the Lamb procedure [28], we write an ansatz for the unknown perturbation of the velocity outside and inside the vesicle [12,19]:

$$\begin{aligned} \mathbf{u} = \sum_{n=0}^{\infty} &\nabla \chi_{-n-1} \times \mathbf{r} + \nabla \phi_{-n-1} - \frac{n-2}{2n(2n-1)} r^2 \nabla p_{-n-1} \\ &+ \frac{n+1}{n(2n-1)} \mathbf{r} p_{-n-1} \end{aligned} \tag{8}$$

and

$$\begin{aligned} \overline{\mathbf{u}} = \sum_{n=0}^{\infty} &\nabla \overline{\chi}_n \times \mathbf{r} + \nabla \overline{\phi}_n + \frac{n+3}{2(n+1)(2n+3)} r^2 \nabla \overline{p}_n \\ &- \frac{n}{(n+1)(2n+3)} \mathbf{r} \overline{p}_n. \end{aligned} \tag{9}$$

The first term expresses vortex motion in a uniform pressure field. The second term represents an irrotational motion which can exist in a uniform pressure field. The last two terms are connected with the pressure distribution ($p = \sum_{n=0}^{\infty} p_n$). The functions $\overline{p}_n$, $\overline{\phi}_n$, and $\overline{\chi}_n$ in the Lamb solution are solid spherical harmonics of order n and $\overline{p}_{-n-1}$, $\overline{\phi}_{-n-1}$, and $\overline{\chi}_{-n-1}$ are solid spherical harmonics of order $-n-1$ [40]. These solid spherical harmonics are determined from the boundary conditions on the membrane: continuity of the velocity field

and the forces at the membrane, and the projected zero divergence of the velocity field [12,19].

Under the linear shear flow only the second-order spherical harmonics functions survive. Hence

$$f = \sum_{m=-2}^{m=2} F_{2m}(t)\mathcal{Y}_2^m(\theta,\phi). \tag{10}$$

Since the motion is analyzed only in the plane of the shear we have $\mathcal{Y}_2^1 = 0$. Therefore, the vesicle dynamics is determined by the components F_{22}, F_{20}, and $F_{2-2} = F_{22}^\star$ (the complex conjugate of F_{22}):

$$f = F_{2-2}\mathcal{Y}_2^{-2} + F_{20}\mathcal{Y}_2^0 + F_{22}\mathcal{Y}_2^2. \tag{11}$$

The area conservation constraint (7) reads

$$\Delta = 4|F_{22}|^2 + 2|F_{20}|^2, \tag{12}$$

and we write the Lamb solution for the total velocity field as

$$\mathbf{v} = \nabla\phi_{-3} + \frac{1}{2}\mathbf{r}p_{-3} + \dot\gamma y\mathbf{e}_x, \tag{13}$$

$$\overline{\mathbf{v}} = \nabla\overline{\phi}_2 + \frac{5}{42}r^2\nabla\overline{p}_2 - \frac{2}{21}\mathbf{r}\overline{p}_2 + \frac{1}{2}\dot\gamma(y\mathbf{e}_x - x\mathbf{e}_y). \tag{14}$$

The shape evolution is determined from the kinematic condition that the interface moves with the normal component of the fluid velocity $\mathbf{v}(r) = \overline{\mathbf{v}}(r) \equiv \mathbf{v}_r$ [13],

$$\frac{\partial r}{\partial t} = \mathbf{v}_r \cdot \mathbf{n}. \tag{15}$$

This equation is obtained, in the usual way, from a transport equation

$$\frac{\partial\varphi}{\partial t} + (\mathbf{v}_r \cdot \nabla)\varphi = 0, \tag{16}$$

where the function φ, which varies continuously, is negative inside the vesicle and positive outside $[\varphi(r,t) = r - 1 - f]$. The kinematic relation (15) should involve $|\nabla(r - f)|$ in the denominator of the left-hand side term.

After lengthy but straightforward algebra, it is found in [12] that the shape parameters F_{2m}, $m = 0,2$, obey (at leading order)

$$\frac{d}{dt}F_{2m} = -i\frac{m}{2}h + i\frac{m}{2}F_{2m} + 2ih\Delta^{-1}(F_{22}^\star - F_{22})F_{2m}. \tag{17}$$

Note that the operator $\frac{d}{dt} - i\frac{m}{2}$ is the Jaumann derivative. The algebra leading to the above equations is technically more involved, and the interested reader can find it in [13,15,19,22–24,30,31]. The evolution in time of the vesicle shape configuration in the plane of the shear is given by the evolution of the F_{22} mode. The out-of-plane deformation along the vorticity direction is described by the F_{20} mode. Condition (12) shows that the maximal extension along the vorticity axis corresponds to $F_{20}^{\max} = \sqrt{\Delta/2}$, and the shape mode F_{22} is equal to zero.

The role of the F_{22} mode can also be clarified by setting

$$F_{22} = \mathcal{R}(t)e^{-2i\psi(t)}, \tag{18}$$

where ψ coincides with the orientation angle of the vesicle and $\mathcal{R}$ is the amplitude of deformation of the vesicle. The parameter $\mathcal{R}$ measures the ellipticity of the vesicle contour in the shear plane. Insertion of (18) into (17), with $m = 2$, and extraction of the real and imaginary parts from (17) lead to (1). This is the line advocated in [12]. Note that the area constraint (12) reads

$$\Delta = 4\mathcal{R}^2 + F_{20}^2, \tag{19}$$

or, equivalently,

$$F_{20}(t) = \pm\sqrt{\frac{\Delta}{2} - 2\mathcal{R}^2(t)}. \tag{20}$$

The area constraint (19) allows us to use a single angle Θ to express the F_{20} mode and the amplitude of the vesicle deformation $\mathcal{R}$:

$$F_{20} = \sqrt{\frac{\Delta}{2}}\sin\Theta \quad \text{and} \quad \mathcal{R} = \frac{\sqrt{\Delta}}{2}\cos\Theta. \tag{21}$$

From (1) and (17) one can easily find

$$\frac{\sqrt{\Delta} - 2\mathcal{R}(t)}{\sqrt{\Delta} + 2\mathcal{R}(t)} = \frac{\sqrt{\Delta} - 2\mathcal{R}(0)}{\sqrt{\Delta} + 2\mathcal{R}(0)}\exp\left(-4h\int_0^t \sin[2\psi(s)]ds\right) \tag{22}$$

and

$$F_{20}(t) = F_{20}(0)\exp\left(-\frac{2h}{\Delta}\int_0^t \cos\Theta(s)\sin[2\psi(s)]ds\right). \tag{23}$$

This indicates in particular that if $F_{20}(0) \neq 0$ the value $F_{20}(t) \neq 0$ for all times and $\mathcal{R} < \sqrt{\Delta}/2$. If $F_{20}(0) = 0$ we have $F_{20}(t) = 0$ for all times (i.e., no deformation along the vorticity direction). In this case the area conservation constraint (12) implies that $\mathcal{R}$ remains constant (shape-preserving regime) and equal to its maximal value $\sqrt{\Delta}/2$. Similarly, if initially $\mathcal{R}(0) = \sqrt{\Delta}/2$, $\mathcal{R}(t) = \sqrt{\Delta}/2$ for all times and then $F_{20} \equiv 0$.

Analogously to F_{22}, the role of F_{20} can also be investigated in the spirit of [13]. On average, the vesicle is elliptical. Instead of $\mathcal{R}$ the deformation can also be quantified by means of the Taylor parameter [3,13,17,19,25] $D = D_{xy} = (r_{\max} - r_{\min})/(r_{\max} + r_{\min})$, where $r_{\max}$ and $r_{\min}$ are the major and the minor axes (in the x-y plane) of the vesicle, respectively. See also [36,37] for capsules. Since

$$\begin{aligned} r_{\max}(t) &= 1 - \frac{1}{4}\sqrt{\frac{5}{\pi}}F_{20}(t) + \sqrt{\frac{15}{32\pi}}\sqrt{\Delta - 2F_{20}^2(t)} \\ &= 1 - \sqrt{\frac{5}{32\pi}}\sqrt{\Delta - 4\mathcal{R}^2(t)} + \sqrt{\frac{15}{8\pi}}\mathcal{R}(t) \end{aligned} \tag{24}$$

and

$$\begin{aligned} r_{\min}(t) &= 1 - \frac{1}{4}\sqrt{\frac{5}{\pi}}F_{20}(t) - \sqrt{\frac{15}{32\pi}}\sqrt{\Delta - 2F_{20}^2(t)} \\ &= 1 - \sqrt{\frac{5}{32\pi}}\sqrt{\Delta - 4\mathcal{R}^2(t)} - \sqrt{\frac{15}{8\pi}}\mathcal{R}(t), \end{aligned} \tag{25}$$

the Taylor vesicle deformation reads

$$D = \sqrt{\frac{15}{32\pi}}\frac{\sqrt{\Delta - 2F_{20}^2(t)}}{1 - \sqrt{5/16\pi}F_{20}(t)}. \tag{26}$$

Note that $D = \sqrt{\frac{15}{8\pi}}\mathcal{R} + O(\mathcal{R}^2)$. The parameter D has been used for a qualitative comparison between vesicle and drop

dynamics [19] and a comparison of the Keller and Skalak theory [1] to the theory of [12] [in which case system (1) is solved numerically]. The Taylor deformation has also been used to infer an evaluation of the membrane shear elastic modulus of artificial capsules with different membranes [32–34] (see also [35]). Recently, the parameter D was used in the study of the dynamics of oblate-shaped capsules [38]. The time-dependent behavior is related to the rate of elongation ($dD/dt > 0$) or compression ($dD/dt < 0$). In [3] the authors developed a simple model that describes the Taylor parameter for giant vesicles as a function of the shear rate (see also [4]).

Using the relation between the Taylor vesicle deformation and the effective excess area Δ_{eff},

$$D = \sqrt{\frac{15\Delta_{\text{eff}}}{32\pi}}, \tag{27}$$

reported by Seifert [4] (see also [3] for giant vesicles), we obtain [13]

$$\Delta_{\text{eff}} = \frac{\Delta - 2F_{20}(t)^2}{[1 - \sqrt{5/16\pi}\,F_{20}(t)]^2}. \tag{28}$$

Note that the parameter Δ_{eff} is time dependent, in contrast to the excess area Δ. This is due to the fluctuations in the F_{20} mode. The effective excess area can be rewritten as

$$\Delta_{\text{eff}} = \frac{\Delta \cos^2\Theta}{(1 - \sqrt{5\Delta/32\pi}\,\sin\Theta)^2}, \tag{29}$$

where Θ is given by (21). Θ is referred to as the shape parameter [21]. This parameter is a measure of how much of the excess area is stored. In Sec. IV, we shall see that the TB-VB transition can be deduced from an analysis of the Taylor parameter D or the effective excess area Δ_{eff}.

As evident from the above discussion, the F_{22} mode provides a convenient basis for describing the vesicle shape configuration under a shear flow in the leading-order theory. Beyond the zero-order approximation [12], the problem is highly nonlinear and difficult to solve analytically. The nonlinear character of (17) is triggered by local membrane incompressibility. Note that this markedly differs from droplet [40,41] and capsule [42] theories where the leading-order equations are linear.

III. MATHEMATICAL FORMULATION AND EXACT SOLUTIONS

As mentioned in the Introduction, we are mainly interested in finding exact expressions of solutions to system (1). One key challenge is that this problem is highly nonlinear. It has been pointed out [12,19] that, unlike the KS equation (see below), it is difficult to obtain all solutions analytically. Therefore, the analytical solution of system (1) presents an open question from the mathematical and physical point of view. In particular, we shall present elementary methods which have been successful in solving system (1) exactly. Our strategy is to have a full understanding of system (1) before including further physical complexity.

In the case of the shape-preserving regime (i.e., $\mathcal{R} \equiv \sqrt{\Delta}/2$), system (1) is reduced to the Jeffery equation

$$\frac{d\psi}{dt} = -\frac{1}{2} + \frac{h}{\sqrt{\Delta}}\cos(2\psi), \tag{30}$$

which simplifies the dynamics. Equation (30) was extensively studied by Keller and Skalak [1]. The vesicle dynamic is described only by the variation of the angle ψ. Two mathematical properties have been noted. If $\frac{\sqrt{\Delta}}{2h} < 1$ ($h > h_c$) Eq. (30) has the following fixed inclination angles (the pure TT regime):

$$\psi_0^{\pm} = \pm\tfrac{1}{2}\arccos(\sqrt{\Delta}/2h). \tag{31}$$

The "+" solution is stable and the "−" solution is unstable. The asymptotic solution is a TT regime. At the critical value $h = h_c$ both fixed inclination angles merge at $\psi = 0$ (saddle-node bifurcation). For $h < h_c$ no fixed inclination angle exists and all solutions to (30) oscillate (TB regime). More precisely, KS showed that the general solution to (30) satisfies

$$\psi(t) = \arctan\left[\frac{-\sqrt{\Delta} + 2h}{\sqrt{\Delta - 4h^2}}\tan\left(\frac{1}{2}\sqrt{1 - 4h^2/\Delta}(t - t_0)\right)\right], \tag{32}$$

where t_0 is a constant (a time at which $\psi = 0$).

It may be understood from the Jeffery equation that we need, for system (1), to distinguish at least two cases for the parameter h: namely, $4h^2 > \Delta$ and $4h^2 < \Delta$. Our approach is not an attempt to introduce another speculative physical scenario, but rather an effort is made to exhibit analytically all physical solutions and to study their dependence (for fixed Δ) on the control parameter h. At first sight system (1) appears to be complicated. The main idea for determining exact analytical solutions is to introduce new coordinates in terms of which system (1) takes a simpler form. Instead of ψ and $\mathcal{R}$ the vesicle dynamics can also be described in terms of the real and imaginary parts of F_{22} ($=\xi - i\zeta$). Accordingly, it is found that system (1) reads

$$\begin{aligned} \frac{d\xi}{dt} &= \zeta\left(1 - \frac{4h}{\Delta}\xi\right), \\ \frac{d\zeta}{dt} &= h - \xi - \frac{4h}{\Delta}\zeta^2. \end{aligned} \tag{33}$$

Note that ξ and ζ are connected to ψ and $\mathcal{R}$ via the relations

$$\xi(t) = \mathcal{R}(t)\cos[2\psi(t)], \quad \zeta(t) = \mathcal{R}(t)\sin[2\psi(t)], \tag{34}$$

so that

$$\psi = \frac{1}{2}\arctan\left(\frac{\zeta}{\xi}\right), \tag{35}$$

and, obviously [in view of (12)],

$$4\mathcal{R}^2 + 2|F_{20}|^2 = \Delta. \tag{36}$$

Very recently a system similar to (33) was derived by Veerapaneni *et al.* [22] when studying the effect of an inclusion on vesicle behavior in shear flow. In this case the leading-order

system for nearly circular vesicle shape is given by

$$\frac{d\xi}{dt} = \zeta\left(1 - \frac{3\beta}{\Delta_l}\xi\right), \qquad \frac{d\zeta}{dt} = \beta - \xi - \frac{3\beta}{\Delta_l}\zeta^2, \tag{37}$$

where β is a function of the inclusion radius and Δ_l is the excess length.

Let us return to our problem. Analogously to system (1), system (33) admits solutions such that $\xi \equiv \frac{\Delta}{4h}$. In this case (33) reduces to the Riccati equation (RE)

$$\frac{d\zeta}{dt} = h - \frac{\Delta}{4h} - \frac{4h}{\Delta}\zeta^2. \tag{38}$$

This equation has the solution

$$\zeta(t) = \frac{\Delta}{4h}\sqrt{\frac{4h^2}{\Delta} - 1}\,\frac{a\exp\left(2\sqrt{\frac{4h^2}{\Delta} - 1}\right)t - 1}{a\exp\left(2\sqrt{\frac{4h^2}{\Delta} - 1}\right)t + 1} \tag{39}$$

if $h > \frac{\sqrt{\Delta}}{2}$, and in the opposite case

$$\zeta(t) = b\tan\left(\sqrt{1 - \frac{4h^2}{\Delta}}(t - t_0)\right), \tag{40}$$

where a, b, and t_0 are real parameters. Having in mind the area conservation constraint (12), the mathematical solution (40) cannot be used to describe the physical problem and has to be ignored; $\zeta(t)$ blows up at a finite time if $b \neq 0$, and if $b = 0$ we have $F_{22} = \frac{\Delta}{4h}$, since $\zeta = 0$. Therfore, $4|F_{22}|^2 = \frac{\Delta^2}{4h^2}$. This contradicts (36), since $h < \frac{\sqrt{\Delta}}{2}$.

The aim of the present section is to obtain all physical solutions. By "physical solution" we mean a solution (ξ,ζ) such that (36) holds. We will proceed by introducing the function

$$\rho = \frac{\xi - h}{\zeta} \tag{41}$$

which is equivalent to the following ansatz:

$$\xi = \zeta\rho + h. \tag{42}$$

In passing, we note that if we assume $\rho \equiv a$, where a is an arbitrary constant, we find from system (33) that a has to be $a = \pm\sqrt{\frac{4h^2}{\Delta} - 1}$, provided $h > h_c$. Qualitatively speaking, a similar condition will appear when considering the general case in which ρ is an arbitrary time-dependent function. From (33) and (41) one deduces

$$\frac{d\rho}{dt} = \rho^2 + 1 - \frac{4h^2}{\Delta}. \tag{43}$$

Equation (43) plays a central role. It shares some analogy with the Jeffery equation (30), in the sense that when $h > h_c$ Eq. (43) has two fixed points $\rho_0 = \pm\sqrt{\frac{4h^2}{\Delta} - 1}$. The "$-$" fixed point is stable and the "$+$" is an unstable one. If $h < h_c$ there is absence of the fixed point and ρ oscillates. Particularly interesting are the explicit expressions of the general solution as follows:

$$\rho(t) = -\omega\frac{e^{\omega t} + C_1 e^{-\omega t}}{e^{\omega t} - C_1 e^{-\omega t}} \tag{44}$$

for $h > h_c$ and for $h < h_c$

$$\rho(t) = \omega\tan(\omega t + C_3), \tag{45}$$

where

$$\omega = \sqrt{\left|1 - \frac{4h^2}{\Delta}\right|} \tag{46}$$

and C_1 and C_3 are constants depending on the initial conditions.

Having found explicit expressions for ρ, one can solve system (33) and analyze analytically the different regimes previously discussed numerically in [12]. Insertion of (44) and (45) into system (33) again results in the ordinary differential equation (nonautonomous RE)

$$\frac{d\zeta}{dt} = -\rho\zeta - \frac{4h}{\Delta}\zeta^2, \tag{47}$$

which can be solved exactly. For $h > h_c$ the functions ζ and ξ have the forms

$$\zeta(t) = \frac{\Delta\omega}{4h}\frac{e^{\omega t} - C_1 e^{-\omega t}}{C_2 + e^{\omega t} + C_1 e^{-\omega t}}, \qquad \xi(t) = \frac{\Delta}{4h} + \frac{\omega^2\Delta}{4h}\frac{C_2}{C_2 + e^{\omega t} + C_1 e^{-\omega t}}, \tag{48}$$

for some constant C_2. Therefore, upon using (34) and (35) the inclination angle and the shape deformation are given by

$$\psi(t) = \frac{1}{2}\arctan\left(\omega\frac{\Delta[e^{\omega t} - C_1 e^{-\omega t}]}{4h^2 C_2 + \Delta[e^{\omega t} + C_1 e^{-\omega t}]}\right) \tag{49}$$

and

$$\mathcal{R}^2(t) = \frac{\Delta^2}{16h^2}\frac{\omega^2(e^{\omega t} - C_1 e^{-\omega t})^2 + (C_2' + e^{\omega t} + C_1 e^{-\omega t})^2}{(C_2 + e^{\omega t} + C_1 e^{-\omega t})^2}, \qquad C_2' = \frac{4h^2}{\Delta}C_2. \tag{50}$$

For $h < h_c$ we have

$$\zeta(t) = \frac{\Delta\omega}{4h}\frac{\cos(\omega t + C_3)}{C_4 + \sin(\omega t + C_3)}, \qquad \xi(t) = \frac{\Delta}{4h}\frac{\Gamma + \sin(\omega t + C_3)}{C_4 + \sin(\omega t + C_3)}, \qquad \Gamma = \frac{4h^2}{\Delta}C_4, \tag{51}$$

where C_4 is a constant depending on the initial conditions;

$$C_4 = \pm\frac{\frac{\Delta}{4h} - \xi(0)}{\sqrt{\omega^2\zeta^2(0) + [\xi(0) - h]^2}}. \tag{52}$$

The above expression is obtained from a simple algebraic manipulation of (51) at $t = 0$.

Using (12) and (51) one sees that $|C_4| \geqslant \frac{\sqrt{\Delta}}{2h}$, and then $|C_4| > 1$ since $h < h_c$. Therefore, the coordinates ξ and ζ are finite for all times and the parameter Γ satisfies

$$|\Gamma| \geqslant \frac{2h}{\sqrt{\Delta}}. \tag{53}$$

The inclination angle and the shape deformation are given, respectively, by

$$\psi(t) = \frac{1}{2}\arctan\left(\omega\frac{\cos(\omega t + C_3)}{\Gamma + \sin(\omega t + C_3)}\right) \tag{54}$$

and

$$\mathcal{R}^2(t) = \frac{\Delta^2}{16h^2}\frac{1}{[C_4 + \sin(\omega t + C_3)]^2}\{\omega^2\cos^2(\omega t + C_3) + [\Gamma + \sin(\omega t + C_3)]^2\}. \tag{55}$$

These may be regarded as the main results of this paper. Without loss of generality we may assume that $C_3 = 0$. Note that the inclination angle and the shape deformation oscillate with the period $T = 2\pi(1 - \frac{4h^2}{\Delta})^{-1/2}$, which decreases with h. We shall see that the present result is an extension of the Keller-Skalak solutions (for rigid particles). Note that $\mathcal{R} = \frac{\sqrt{\Delta}}{2}$ (shape-preserving regime) if and only if

$$\Gamma = \pm\Gamma_c, \tag{56}$$

where

$$\Gamma_c = \frac{2h}{\sqrt{\Delta}} < 1. \tag{57}$$

Note that if $|\Gamma| < \Gamma_c$ the mathematical solutions (49) and (50) have to be ignored.

IV. VESICLE DYNAMICS

In this section we discuss in more detail the different regimes described by the above exact solutions. In particular, we analyze the effect of the parameter Γ on the TB and VB behaviors and derive a basin of attraction for each regime.

A. Tank-treading solutions ($h > \frac{\sqrt{\Delta}}{2}$)

Since the argument of the arctangent function in (49) goes to ω as t tends to infinity, where ω is given by (46), expression (49) shows that ψ tends to

$$\psi(\infty) = \frac{1}{2}\arctan\left[\frac{4h^2 - \Delta}{\Delta}\right]^{1/2} = \psi_0^+ \tag{58}$$

as t approaches infinity, where ψ_0^+ is given by (31) (see expression (28) of [19]). In addition, we note that $\mathcal{R}(t)$ goes to $\frac{\sqrt{\Delta}}{2}$ as t tends to infinity. That is to say the asymptotic solution corresponds to a TT solution.

As noted in [19] if $\Delta = 0$ (sphere) the orientation angle is $\pi/4$ (the orientation of maximum straining); otherwise the orientation angle is always smaller than $\pi/4$. A nonzero value of the excess area allows vesicle deformation.

For completeness, we note that $\psi(t)$ tends to a finite limit as t tends to $-\infty$,

$$\psi(-\infty) = -\frac{1}{2}\arctan\left[\frac{4h^2 - \Delta}{\Delta}\right]^{1/2} = \psi_0^-, \tag{59}$$

where ψ_0^- is given by (31). In addition, if C_1 and C_2 are positive the inclination angle ψ is monotonically increasing and thus satisfies

$$\psi_0^- < \psi < \psi_0^+ \tag{60}$$

for all times. It is worth noticing that, in the TT regime, any solution to system (33) is in fact, a kink solution which connects the unstable fixed point at $-\infty$ to the stable one at ∞. Expression (48) provides a simple explicit expression for a kink (vertical) solution satisfying (60):

$$\xi(t) = \frac{\Delta}{4h}, \quad \zeta(t) = \frac{\Delta\omega}{4h}\frac{e^{\omega t} - e^{-\omega t}}{e^{\omega t} + e^{-\omega t}}. \tag{61}$$

The inclination angle and the shape deformation read

$$\psi(t) = \frac{1}{2}\arctan\left(\omega\frac{e^{\omega t} - e^{-\omega t}}{e^{\omega t} + e^{-\omega t}}\right), \qquad \mathcal{R}^2(t) = \left(\frac{\Delta}{4h}\right)^2\left[1 + \omega^2\frac{(e^{\omega t} - e^{-\omega t})^2}{(e^{\omega t} + e^{-\omega t})^2}\right]. \tag{62}$$

As the viscosity ratio λ approaches the critical value λ_c given by (2), or equivalently $4h^2 = \Delta$, both inclination angles $\psi_0^{\pm}$ vanish and all solutions of system (33) merge at $(\xi,\zeta) = (\sqrt{\Delta}/2,0)$. Above λ_c we shall see that our results describe two types of periodic solution.

Finally, we note that the constants C_1 and C_2, which depend on the initial conditions, have to be selected such that the area conservation constraint (12) is satisfied for all times. In fact, system (33) admits solutions which blow up at a finite time or which connect the unstable fixed point to $(h,0)$, which is the third fixed point. However, those solutions have to be ignored. The fixed point $(h,0)$ violates the area conservation constraint (12) for $h > h_c$. We are implicitly assuming that our explicit exact solutions satisfy (12) for both cases $h > h_c$ and $h < h_c$. In fact, the constraint (12) demands that the quantity $\xi^2(0) + \zeta^2(0)$ is not larger than $\Delta/4$ [see (36)]. In Fig. 1 we present some trajectories in the phase plane (ξ,ζ) subject to the initial conditions

$$-\sqrt{\Delta}/2 \leqslant \xi(0) \leqslant \sqrt{\Delta}/2, \quad \zeta(0) = 0. \tag{63}$$

The initial inclination angle is fixed to take the value $\psi(0) = 0$. This is a simple strategy for obtaining a physically acceptable

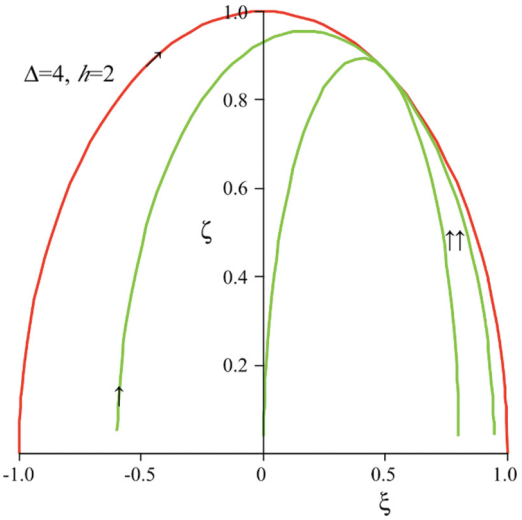

FIG. 1. (Color online) Trajectories of (33) in phase space (ξ,ζ). Here the parameters are $h = 2$ and $\Delta = 4$ for simplicity. All trajectories tend to $\frac{1}{2}(1,\sqrt{3})$ as t approaches infinity.

solution. We then vary the initial condition $\xi(0)$ to generate a family of distinct solutions.

B. Tumbling and vacillating-breathing solutions: Dependence on the TB-VB parameter

We turn now to the most interesting and rich case $h < h_c$. As mentioned before, Misbah [12] presented numerical solutions to system (1) showing that the VB mode coexists with the TB mode, and the mode selection is determined by the initial conditions.

Below, we shall analyze the different closed orbits that emerge from (54). We shall attempt to identify exactly the initial conditions and the parameter Γ that lead to the TB or VB regime. We recall, using (51) and (52), that Γ is given by

$$\Gamma = \pm\frac{4h^2}{\Delta}\frac{\frac{\Delta}{4h} - \xi(0)}{\sqrt{\omega^2\zeta^2(0) + [\xi(0) - h]^2}}. \tag{64}$$

Naively, we may suggest that the inclination angle is written as ($C_3 = 0$)

$$\psi(t) = \frac{1}{2}\arctan\left(\omega\frac{\cos\omega t}{\Gamma + \sin\omega t}\right) \tag{65}$$

for all times. In this case ψ oscillates in the interval $[-\pi/4,\pi/4]$ and then cannot describe any TB solution. Expression (65) has to be refined. In passing, we note that $(-\mathcal{R},\psi \pm \pi/2)$ are solutions of system (1) as well as $(\mathcal{R},\psi)$. For a rigorous mathematical and physical proof the inclination angle will be defined by

$$\psi(t) = \begin{cases} \frac{1}{2}\arctan\left(\omega\frac{\cos\omega t}{\Gamma+\sin\omega t)}\right) & \text{if} \quad \xi > 0, \\ -\frac{\pi}{2} + \frac{1}{2}\arctan\left(\omega\frac{\cos\omega t}{\Gamma+\sin\omega t)}\right) & \text{if} \quad \xi < 0,\ \zeta < 0, \\ +\frac{\pi}{2} + \frac{1}{2}\arctan\left(\omega\frac{\cos\omega t}{\Gamma+\sin\omega t)}\right) & \text{if} \quad \xi < 0,\ \zeta > 0. \end{cases} \tag{66}$$

In the above expression the inclination angle is defined as the principal value of the real arctangent function which is the unique solution to

$$\begin{aligned} \cos[2\psi(t)] &= \frac{\xi(t)}{\sqrt{\xi^2(t) + \zeta^2(t)}}, \\ \sin[2\psi(t)] &= \frac{\zeta(t)}{\sqrt{\xi^2(t) + \zeta^2(t)}}, \end{aligned} \tag{67}$$

satisfying $-\pi \leqslant 2\psi(t) \leqslant +\pi$. The inclination angle jumps discontinuously from $-\pi/2$ to $+\pi/2$ at $\xi < 0$ and $\zeta = 0$. The inclination angle can be written, for convenience, in the form

$$\begin{aligned} \psi(t) = {} & \frac{\pi}{4}\frac{\Gamma}{|\Gamma|}\frac{\cos\omega t}{|\cos\omega t|}\left[1 - \frac{\Gamma}{|\Gamma|}\frac{\Gamma + \sin\omega t}{|\Gamma + \sin\omega t|}\right] \\ & + \frac{1}{2}\arctan\left(\omega\frac{\cos\omega t}{\Gamma + \sin\omega t}\right). \end{aligned} \tag{68}$$

Three cases are clearly identified.

For $|\Gamma| > 1$ the function $t \to \chi(t) = \Gamma + \sin\omega t$ never vanishes and then $\xi(t)$ is positive for all times. Therefore, the orientation angle satisfies (65) for all times. Consequently, the vesicle exhibits the VB mode to which its inclination angle oscillates between the minimal angle $\psi_{\mathrm{vb}-} = -\frac{1}{2}\arctan\left(\frac{\omega}{\sqrt{\Gamma^2-1}}\right)$ and the maximal angle $\psi_{\mathrm{vb}+} = +\frac{1}{2}\arctan\left(\frac{\omega}{\sqrt{\Gamma^2-1}}\right)$. Both minimal and maximal angles satisfy $0 < |\psi_{\mathrm{vb}\pm}| < \pi/4$. Recall that the vesicle undergoes periodic shape deformation. This is a signature of the a VB regime (see the solid red line of Fig. 2).

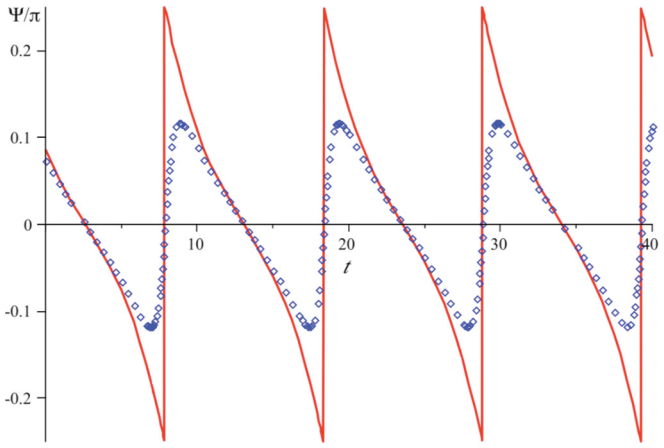

FIG. 2. (Color online) Dynamics of the inclination angle ψ for vacillating-breathing modes. Parameters are $\Delta = 4$ and $h = 0.8$ ($\Gamma_c = 0.8$). $\Gamma = 1.2$ for the square blue line and 1 for the solid red line (separatrix mode).

For $|\Gamma| = 1$ the function χ is non-negative and vanishes at finite times. Therefore, the inclination angle ψ spans the whole range $[-\pi/4,\pi/4]$ [see Fig. 2 (square blue line)]. In particular, ψ reaches $\pm\pi/4$.

For $\Gamma_c \leqslant |\Gamma| < 1$ the function ξ changes sign and then ψ oscillates between $\pm\pi/2$. This is a TB regime, and the solution is given by (68). An example of this motion can be seen in Fig. 3. Clearly, the parameter Γ can be identified as the tumbling- or vacillating-breathing parameter. The variation of the inclination angle is reported in Figs. 2 and 3 in agreement with numerical solutions reported in the literature.

From the above discussion one deduces that the border separating the VB and TB modes is obtained analytically from

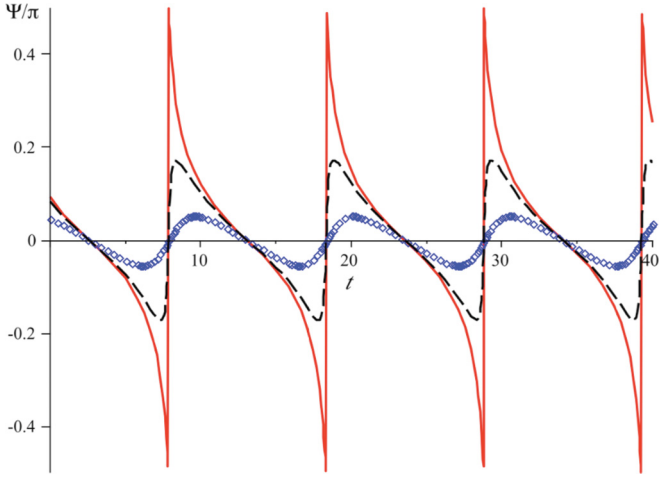

FIG. 3. (Color online) Dynamics of the inclination angle ψ/π depending on the parameter Γ, for $h = 0.8$ and $\Delta = 4$ ($\Gamma_c = 0.8$). Tumbling mode (solid red line) for $\Gamma = 0.9$ and vacillating-breathing mode for $\Gamma = 2$ (square blue line) and $\Gamma = 1.05$ (dashed black line). The period is $T = \frac{10}{3}\pi$.

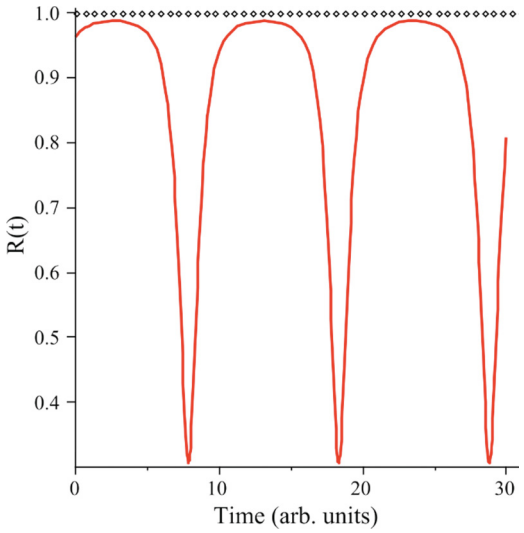

FIG. 4. (Color online) The amplitude $\mathcal{R}(t)$ for $h = 0.8$ and $\Delta = 4$ ($\Gamma_c = 0.8$), in the tumbling regime for $\Gamma = 0.9$. In the VB regime the behavior is similar. The shape-preserving regime ($\Gamma_c = 0.8$) is plotted as the square black line for comparison.

the equation $\Gamma^2 = 1$, which is equivalent to

$$\xi(0)\left[2h - \left(1 + \frac{4h^2}{\Delta}\right)\xi(0)\right] = \zeta^2(0). \tag{69}$$

In passing, we point out that if initially the vesicle configuration satisfies (69) then the relation

$$\xi(t)\left[2h - \left(1 + \frac{4h^2}{\Delta}\right)\xi(t)\right] = \zeta^2(t) \tag{70}$$

holds for all times. The orientation angle of the border mode can be expressed as

$$\psi(t) = \frac{1}{2}\arctan\left(\omega\frac{\cos(\omega t + 3\pi/2)}{1 + \sin(\omega t + 3\pi/2)}\right) \tag{71}$$

or, equivalently,

$$\psi(t) = -\frac{1}{2}\arctan\left[\omega\tan\left(\frac{1}{2}\omega(t - t_1)\right)\right], \tag{72}$$

where t_1 is a constant. It is interesting to note that the TB motion has a strong similarity with the border-separating motion. Figures 2 and 3 show solutions (angle as a function of time) for the same parameters h and Δ, but with a parameter $\Gamma = 1$ for the separatrix mode and $\Gamma_c \leqslant |\Gamma| < 1$ for the TB mode. In Fig. 4 we show a typical behavior for the amplitude $\mathcal{R}(t)$ for $|\Gamma| > \Gamma_c$. Recall that the critical case $|\Gamma| = \Gamma_c$ corresponds to the shape-preserving regime.

Note that system (1) admits TB solutions with $|\Gamma| < \Gamma_c$; however, these mathematical solutions are physically unacceptable. The area conservation constraint (12) is violated.

Now, we present interesting results confirming the role of the TB-VB parameter. First, we can deduce from (12) and (55) the expression for the F_{20} mode:

$$F_{20}(t) = \pm\omega\frac{\Delta}{2\sqrt{2}h}\sqrt{\frac{\Delta}{4h^2}\Gamma^2 - 1}\,\frac{1}{\frac{\Delta}{4h^2}\Gamma + \sin\omega t}. \tag{73}$$

In passing we note that if $|\Gamma| = \Gamma_c$ we have $F_{20}(t) = 0$ for all times; a fixed ellipsoid shape. This is the situation we are going to deal with in the next section. Recall that F_{20} never vanishes if $F_{20}(0) \neq 0$ (see Sec. II). Therefore, we may assume without loss of generality that F_{20} is positive, and then $\Gamma > 0$.

Equation (73) shows that the maximum deformation of F_{20} is

$$F_{20}^{\mathrm{m}} = \omega\frac{\Delta}{2\sqrt{2}h}\sqrt{\frac{\Delta}{4h^2}\Gamma^2 - 1}\,\frac{1}{\frac{\Delta}{4h^2}\Gamma - 1} \leqslant \sqrt{\frac{\Delta}{2}}. \tag{74}$$

Interestingly, the maximum extension along the vorticity axis, $\sqrt{\frac{\Delta}{2}}$, is attained if and only if $\Gamma = 1$ (the separatrix mode). From this we observe that the Taylor parameter D attains zero at its minimum [see (26)]. That is to say, if $|\Gamma| = 1$ the vesicle attains a circular shape in the plane shear. A detailed analysis of this case will be reported elsewhere.

One of the results that emerges from this analysis is that for $h < h_c$ our approach introduces the TB-VB parameter Γ which may play the role of a control parameter. $\Gamma = \Gamma_c$ corresponds to a KS tumbling solution (rigid particle), the range $\Gamma_c < \Gamma < 1$ leads to tumbling motions with deformable shape, and the range $\Gamma > 1$ corresponds to vacillating-breathing modes. The TB-VB transition occurs if $\Gamma = 1$, leading to a circular shape in the shear plane (over one period).

C. Keller-Skalak theory

The task of the present section is to compare our results with the TB prediction obtained by KS. In fact, a natural wish would be to understand how a KS tumbling solution can be derived from (68) if the ellipsoid shape is fixed. In this case we have $\Gamma = \pm\Gamma_c$ [see (56)] and then $C_4 = \Gamma_c^{-1}$.

We assume without loss of generality that $\Gamma = \Gamma_c$. First, we easily check, for $\xi < 0$ and $\zeta > 0$, that the inclination angle ψ reads

$$\psi(t) = \frac{\pi}{2} + \arctan\left(\frac{\omega\cos(\omega t)}{\Gamma_c + \sin\omega t - \sqrt{(\Gamma_c + \sin\omega t)^2 + \omega^2\cos^2\omega t}}\right), \tag{75}$$

by using the identity $\frac{1}{2}\arctan x = \arctan\frac{x}{1+\sqrt{1+x^2}}$. Next, using (55) the quantity $(\Gamma_c + \sin\omega t)^2 + \omega^2\cos^2\omega t$ is replaced by $\frac{4h^2}{\Delta}(\Gamma_c^{-1} + \sin\omega t)^2$. It follows from this that the inclination angle can be written as

$$\psi(t) = \frac{\pi}{2} + \arctan\left(\frac{\omega\cos\omega t}{\left(\frac{2h}{\sqrt{\Delta}} - 1\right)(1 - \sin\omega t)}\right). \tag{76}$$

Therefore, there exists a real t_0 ($\sin\omega t_0 = 1$) such that

$$\psi(t) = \frac{\pi}{2} + \arctan\left(\frac{\omega}{\frac{2h}{\sqrt{\Delta}} - 1}\Big/\tan\frac{\omega}{2}(t - t_0)\right), \tag{77}$$

and this coincides with the KS solution (32). Similar results are obtained for the case $\xi > 0$ and the case $\xi < 0$ and $\zeta < 0$. Note that our solution in the TB regime coincides with the KS one only if $\mathcal{R}$ is constant (shape-preserving solution); otherwise the general solution is given by (68), due to the

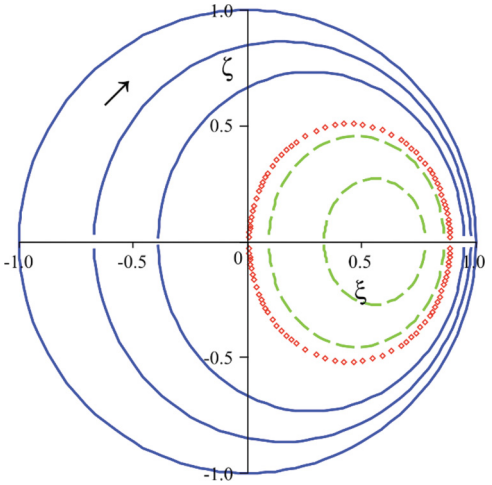

FIG. 5. (Color online) Phase portrait of system (33) for $h < \sqrt{\Delta}/2 = 1$, showing vacillating-breathing vesicle (dashed green lines) and tumbling vesicle (solid blue lines). The square red orbit which goes through the origin is the separatrix mode.

fact that the shape evolves in times (the short and long axes oscillate in time).

V. BASIN OF EACH REGIME

In the course of the investigation we mentioned that a physical solution has to satisfy the area conservation constraint (7). Thus the physical region or the physical basin of attraction of $\frac{\Delta}{4h}(1,\sqrt{\frac{4h^2}{\Delta}-1})$ (for the TT regime) is naturally $\mathcal{B}_{tt} = \mathcal{D}$, where $\mathcal{D}$ is the disk defined by

$$\mathcal{D} = \left\{(\xi(0),\zeta(0));\ \xi^2(0)+\zeta^2(0) \leqslant \frac{\Delta}{4}\right\}. \tag{78}$$

For $\Delta > 4h^2$, as shown above, the TB and VB modes coexist and are distinguished according to the values of the parameter Γ which depends on the initial condition $(\xi(0),\zeta(0))$, as well as the fixed excess area and the ratio viscosity (see Fig. 5).

Let $\mathcal{P}$ be the closed orbit [see (70)]

$$\mathcal{P} = \left\{(\xi,\zeta) \in \mathbb{R}^2 : \xi\left[2h - \left(1+\frac{4h^2}{\Delta}\right)\xi\right] = \zeta^2\right\}, \tag{79}$$

which goes through the origin. Recall that $\mathcal{P}$ defines a "separatrix mode," or a boundary delimiting the TB and VB regimes (see the square red line of Fig. 5). The exact basin of the VB mode, $\mathcal{B}_{\mathrm{vb},h}$, is the bounded open domain with the boundary $\mathcal{P}$:

$$\mathcal{B}_{\mathrm{vb},h} = \left\{(\xi,\zeta) \in \mathbb{R}^2 : |\zeta| < \sqrt{\xi\left[2h - \left(1+\frac{4h^2}{\Delta}\right)\xi\right]}\right\}, \tag{80}$$

while the exact basin of the TB mode is given by $\mathcal{B}_{\mathrm{tb},\lambda} = \mathcal{D} \setminus \mathcal{B}_{\mathrm{vb},h}$ ($\mathcal{D}$ excluding $\mathcal{B}_{\mathrm{vb},h}$); see Fig. 6.

To explore the VB-TB boundary we assume that $\xi(0) > 0$ and $0 < \xi^2(0)+\zeta^2(0) < \Delta/4$. By varying h from h_c to 0 (by increasing the viscosity contrast λ from λ_c to ∞), one sees that there exists, as expected [19], a second critical value of h_c' ($<h_c$) where the VB solution disappears at $h = h_c'$ and where only the TB is the attracting solution (the coexistence between the VB and TB modes disappears). The second critical value h_c' can be determined as the root of Eq. (69); that is,

$$h_c' = \frac{\Delta}{4\xi(0)}\left[1 - \sqrt{1 - \frac{4}{\Delta}[\xi^2(0)+\zeta^2(0)]}\right]. \tag{81}$$

Equation (69) has two roots. Only the root (81) is physically acceptable ($h_c' < \sqrt{\Delta}/2$). The VB regime disappears in favor of tumbling (marginal stability of the separatrix VB mode). The VB mode is an intermediate regime between the TT and TB modes (it coexists with TB in the range $h_c' < h < h_c$, while for $h < h_c'$, only the TB regime survives). However, if $\xi^2(0)+\zeta^2(0) = \Delta/4$, or if $\xi(0)$ is negative, there is no intermediate regime. The transition from the TT to the TB

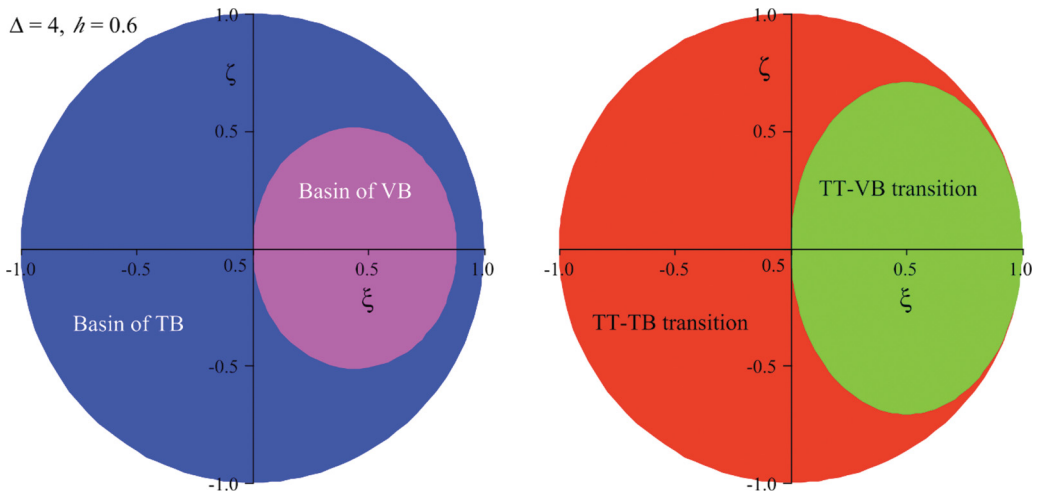

FIG. 6. (Color online) Basin of each regime for given h and Δ parameters (left) and a typical localization of the TT-TB and TT-VB transition regions (right).

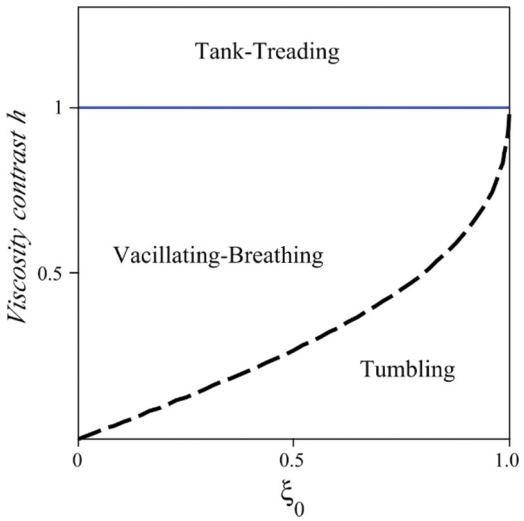

FIG. 7. (Color online) A phase diagram representing the three regimes TT, VB, and TB in the $[\xi(0)=\xi_0,h]$ plane for $\Delta=4$. We see that the VB width decreases with increasing ξ_0 and vanishes at $\xi_0=\sqrt{\Delta}/2$ (KS solution). The dashed black line (TB-VB transition) shows the evolution of the second critical value h_c' as a function of $\xi_0=\xi(0)$.

regime is direct. Actually, the the transition region from the TT to the VB regime is given by (see Fig. 6)

$$\mathcal{D}_c=\left\{(\xi,\zeta)\in\mathbb{R}^2:|\zeta|<\sqrt{\xi[\sqrt{\Delta}-2\xi]}\right\}. \tag{82}$$

The phase diagram of Fig. 7 represents the TB and VB regimes as a function of the parameters h and $\xi(0)>0$ for $\zeta(0)=0$ and a given Δ. Figure 7 also shows that for $0<\xi(0)<\frac{\sqrt{\Delta}}{2}$ the TB and VB regimes are always present. Each has its own basin of attraction. As expected, the VB mode occurs in the vicinity of the transition from the TT to the TB regime, for $0<\xi<\sqrt{\Delta}/2$. The VB width, defined as the difference between the critical value and the second critical value of h, is given by, for $0<\xi(0)<\frac{\sqrt{\Delta}}{2}$ and $\zeta(0)=0$,

$$\Delta h=\frac{\sqrt{\Delta}}{2}\left[1-\frac{\sqrt{\Delta}}{2\xi(0)}\left(1-\sqrt{1-\frac{4}{\Delta}\xi^2(0)}\right)\right], \tag{83}$$

which goes to 0 as $\xi(0)$ tends to $\frac{\sqrt{\Delta}}{2}$ (KS solution).

Finally, we note that our explicit solutions allow us to evaluate the limit of the amplitude of the VB mode as h tends to h_c. The VB angular amplitude $\Delta\psi_{\rm vb}$ [defined as the difference between the maximum and the minimum of $\psi(t)$], is given by

$$\Delta\psi_{\rm vb}=\arctan\frac{\sqrt{\omega^2\zeta^2(0)+[\xi(0)-h]^2}}{\sqrt{\xi(0)\left[2h-\left(1+\frac{4h^2}{\Delta}\right)\xi(0)\right]-\zeta^2(0)}} \tag{84}$$

for $h_c'<h<h_c$, where h_c' is given by (81) (the threshold of the TB-VB transition). When the parameter h tends to the threshold value of the TB-VB transition we have $\lim_{h\uparrow h_c}\Delta\psi_{\rm vb}=0$. This result shows analytically that the amplitude $\Delta\psi_{\rm vb}$ approaches zero at the TT-VB boundary in a continuous manner [24]. More precisely, we have $\Delta\psi_{\rm vb}\sim\sqrt{h_c-h}$ as $h\to h_c$, a prototypical result for a supercritical (or pitchfork) bifurcation.

VI. CONCLUSION

We have investigated system (1) derived in Ref. [12] to describe the dynamics of vesicles under a shear flow in the small deformation regime. Our approach, which has a remarkable degree of simplicity, leads to exact solutions for the vesicle orientation in the flow and its shape evolution. As a result, three different types of motion have been explicitly identified (TT, TB, and VB) depending on the viscosity contrast and the excess area. In particular, for $h<h_c$, the coexistence of the TB and VB regimes is most clearly observed in the following exact orientation angle [see (68)]:

$$\psi(t)=\frac{\pi}{4}\frac{\cos\omega t}{|\cos\omega t|}\left[1-\frac{\Gamma+\sin\omega t}{|\Gamma+\sin\omega t|}\right]+\frac{1}{2}\arctan\left(\omega\frac{\cos\omega t}{\Gamma+\sin\omega t}\right), \tag{85}$$

where the TB-VB parameter Γ, which is assumed to be positive, ranges from $\frac{2h}{\sqrt{\Delta}}$ to ∞ (for a physical meaning). The TB and VB modes and the TB-VB transition are predicted as functions of the control parameter Γ. If $\frac{2h}{\sqrt{\Delta}}\leqslant\Gamma<1$ we have the TB regime, whereas if $\Gamma\geqslant 1$ the VB regime occurs. Our results allow us to locate the border separating the TB and VB regimes, or the TB-VB transition. This occurs if $\Gamma=1$. In this case the vesicle momentarily attains a circular shape in the shear plane. In addition, the present results are used to evaluate the VB angular amplitude and to recover the KS solutions in the shape-preserving limit, or equivalently $\Gamma=\frac{2h}{\sqrt{\Delta}}$. The exact closed solutions may provide a more elegant and simple way of analyzing the apparent viscosity of a dilute suspension of vesicles as well as the normal stress effects. These questions are currently under investigation. Finally, the present results can be used in order to reexamine the incompressible capsule model considered recently [21,23], where the evolution equations reduce exactly to system (1) when the shear elasticity is set equal to zero. Thus, our present solutions can be used as a starting basic solution, in order to treat the elasticity effect perturbatively. Similarly, the present solutions can be used in order to study systems of vesicle evolution equations that take into account higher-order terms [15,16].

ACKNOWLEDGMENTS

M.G., M.A., and M.B. acknowledge support by FEDER (Fond Européen de Développement Régional) and the Conseil Régional de Picardie, Project MODCAP. C.M. is grateful to CNES (Centre National d'Etudes Spatiales) and ESA (European Space Agency) for financial support.

[1] S. R. Keller and R. Skalak, J. Fluid Mech. **120**, 27 (1982).
[2] M. Kraus, W. Wintz, U. Seifert, and R. Lipowsky, Phys. Rev. Lett. **77**, 3685 (1996).
[3] K. H. de Haas, C. Blom, D. van den Ende, M. H. G. Duits, and J. Mellema, Phys. Rev. E **56**, 7132 (1997).
[4] U. Seifert, Eur. Phys. J. B **8**, 405 (1999).
[5] T. Biben and C. Misbah, Phys. Rev. E **67**, 031908 (2003).
[6] J. Beaucourt, F. Rioual, T. Séon, T. Biben, and C. Misbah, Phys. Rev. E **69**, 011906 (2004).
[7] F. Rioual, T. Biben, and C. Misbah, Phys. Rev. E **69**, 061914 (2004).
[8] H. Noguchi and G. Gompper, Phys. Rev. Lett. **93**, 258102 (2004).
[9] V. Kantsler and V. Steinberg, Phys. Rev. Lett. **95**, 258101 (2005).
[10] V. Kantsler and V. Steinberg, Phys. Rev. Lett. **96**, 036001 (2006).
[11] M. A. Mader, V. Vitkova, M. Abkarian, A. Viallat, and T. Podgorski, Eur. Phys. J. E **19**, 389 (2006).
[12] C. Misbah, Phys. Rev. Lett. **96**, 028104 (2006).
[13] P. M. Vlahovska and R. S. Gracia, Phys. Rev. E **75**, 016313 (2007).
[14] G. Danker and C. Misbah, Phys. Rev. Lett. **98**, 088104 (2007).
[15] G. Danker, T. Biben, T. Podgorski, C. Verdier, and C. Misbah, Phys. Rev. E **76**, 041905 (2007).
[16] V. V. Lebedev, K. S. Turitsyn, and S. S. Vergeles, Phys. Rev. Lett. **99**, 218101 (2007).
[17] H. Noguchi and G. Gompper, Phys. Rev. Lett. **98**, 128103 (2007).
[18] V. Vitkova, M. A. Mader, B. Polack, C. Misbah, and T. Podgorski, Biophys. J. **95**, L33 (2008).
[19] G. Danker, C. Verdier, and C. Misbah, J. Non-Newtonian Fluid Mech. **152**, 156 (2008).
[20] J. Deschamps, V. Kantsler, and V. Steinberg, Phys. Rev. Lett. **102**, 118105 (2009).
[21] R. Finken, S. Kessler, and U. Seifert, J. Phys.: Condens. Matter **23**, 184113 (2011).
[22] S. K. Veerapaneni, Y. N. Young, P. M. Vlahovska, and J. Blawzdziewicz, Phys. Rev. Lett. **106**, 158103 (2011).
[23] P. M. Vlahovska, Y. N. Young, G. Danker, and C. Misbah, J. Fluid Mech. **668**, 221 (2011).
[24] B. Kaoui, A. Farutin, and C. Misbah, Phys. Rev. E **80**, 061905 (2009).
[25] P. Bagchi and R. M. Kalluri, Phys. Rev. E **81**, 056320 (2010).
[26] A. Farutin, T. Biben, and C. Misbah, Phys. Rev. E **81**, 061904 (2010).
[27] E. Maitre, C. Misbah, P. Peyla, and A. Raoult, Physica D **241**, 1146 (2012).
[28] H. Lamb, *Hydrodynamics*, 6th ed. (Cambridge University Press, Cambridge, England, 1932).
[29] R. G. Cox, J. Fluid Mech. **37**, 601 (1969).
[30] V. V. Lebedev, K. S. Turitsyn, and S. S. Vergeles, New J. Phys. **10**, 043044 (2008).
[31] J. T. Schwalbe, P. M. Vlahovska, and M. J. Miksis, Phys. Rev. E **83**, 046309 (2011).
[32] D. Barthès-Biesel, Curr. Opin. Colloid Interface Sci. **16**, 3 (2011).
[33] K. S. Chang and W. L. Olbricht, J. Fluid Mech. **250**, 587 (1993).
[34] A. Walter, H. Rehage, and H. Leonhard, Colloid Polym. Sci. **278**, 169 (2000).
[35] E. Lac and D. Barthès-Biesel, Phys. Fluids **17**, 072105 (2005).
[36] E. Foessel, J. Walter, A.-V. Salsac, and D. Barthès-Biesel, J. Fluid Mech. **672**, 477 (2011).
[37] J. Walter, A.-V. Salsac, and D. Barthès-Biesel, J. Fluid Mech. **676**, 318 (2011).
[38] P. Bagchi and R. M. Kalluri, Phys. Rev. E **80**, 016307 (2009).
[39] V. Kantsler and V. Steinberg, Phys. Rev. Lett. **96**, 036001 (2006).
[40] G. Cox, J. Fluid Mech. **37**, 601 (1961).
[41] N. A. Frankel and A. Acrivos, J. Fluid Mech. **44**, 65 (1970).
[42] D. D. Barthès-Biesel and J. M. Rallison, J. Fluid Mech. **113**, 251 (1981).